Tectonophysics 811 (2021) 228874

Contents lists available at ScienceDirect

Tectonophysics

journal homepage: www.elsevier.com/locate/tecto

Crustal velocity structure of Cathaysia Block from an active-source seismic profile between Wanzai and Hui'an in SE China

Jiyan Lin [a,b,f], Tao Xu [a,g,*], Huiteng Cai [c,**], Qingtian Lü [d], Zhiming Bai [a], Yangfan Deng [e], Yongqian Zhang [d], Minfu Huang [a,f], José Badal [h], Xing Jin [c]

[a] State Key Laboratory of Lithospheric Evolution, Institute of Geology and Geophysics, Chinese Academy of Sciences, Beijing 100029, China
[b] Geophysical Exploration Center, China Earthquake Administration, Zhengzhou 450002, China
[c] Earthquake Administration of Fujian Province, Fuzhou 350003, China
[d] Institute of Mineral Resources, Chinese Academy of Geological Sciences, Beijing 100037, China
[e] State Key Laboratory of Isotope Geochemistry, Guangzhou Institute of Geochemistry, Chinese Academy of Sciences, Guangzhou 510640, China
[f] University of Chinese Academy of Sciences, Beijing 100049, China
[g] Innovation Academy for Earth Science, Chinese Academy of Sciences, Beijing 100029, China
[h] Physics of the Earth, Sciences B, University of Zaragoza, Pedro Cerbuna 12, Zaragoza 50009, Spain

ARTICLE INFO

Keywords:
Wide-angle reflection and refraction
P-wave velocity structure
Tectonic boundaries
Cathaysia
SE China

ABSTRACT

With the purpose of exploring the widely distributed Mesozoic granitoids in SE China and the related mineralization, we carried out a new 530-km-long seismic wide-angle reflection and refraction (WARR) profile along the transect Wanzai- Hui'an. Based on a previous exploration in 2012 and the analysis of this WARR profile, we have deduced a detailed P-wave velocity model of the crust and uppermost mantle. The main results are: (1) The crustal thickness is about 30 to 32 km beneath the Yangtze Block and West Cathaysia, and 29 to 30 km below the East Cathaysia, which represents a significant thinning with respect to the worldwide average thickness of shields and platforms. (2) The variation in seismic velocity between the upper crust and middle-lower crust in the Yangtze Block and the Cathaysia Blocks indicates that the Shaoxing-Jiangshan-Pingxiang Fault (SJPF) is the tectonic boundary between the Yangtze and Cathaysia and the Zhenghe-Dapu Fault (ZDF) is the tectonic boundary between the west and east Cathaysia. (3) The middle crust exhibits a low P-wave velocity layer of 6.2 km/s below the Wuyishan Metallogenic Belt (WMB). This low velocity layer can be attributed to the delamination during the Caledonian orogeny and the Yanshanian extension. (4) The middle-lower crust shows a clear lateral velocity variation from west to east in Cathaysia. The subduction of the Paleo-Pacific plate is believed to be the main reason for the extensional tectonic environment and magmatism during the Yanshanian (Jurassic-Cretaceous) period, leading to significant crustal and lithospheric thinning. Relatively high velocity in the middle-lower crust and widely disseminated Cretaceous volcanic rocks in East Cathaysia may be related to the slab rollback of the Paleo-Pacific plate in the late Yanshanian (Cretaceous) period.

1. Introduction

Since the Neoproterozoic, the amalgamation of the Yangtze and the Cathaysia formed the South China mainland whose easternmost part (Fig. 1) is characterized by the widely distributed Mesozoic granitoids and abundant mineral resources (Zhou et al., 2006; Li and Li, 2007; Mao et al., 2011; Wang et al., 2013; Mao et al., 2014). Granitoids can be classified into belts according to their ages and distributions. For instance, Indosinian (251–205 Ma) granitoids are scattered throughout West Cathaysia, outcropping in small areas and showing structures related to collisional frame (Fig. 1). Granitoid-volcanic rocks of the Early Yanshanian (180–142 Ma) period are distributed throughout West Cathaysia in zones parallel to the coastline, associated with the origin of the rift and the partial melting of the crust. Granitoid-volcanic rocks of the Late Yanshanian (142–67 Ma) period are scattered throughout East Cathaysia, revealing a southeast migration towards the ocean, with

* Corresponding author at: State Key Laboratory of Lithospheric Evolution, Institute of Geology and Geophysics, Chinese Academy of Sciences, Beijing 100029, China.
** Corresponding author.
E-mail addresses: xutao@mai.iggcas.ac.cn (T. Xu), caihuiteng@126.com (H. Cai).

https://doi.org/10.1016/j.tecto.2021.228874
Received 12 July 2020; Received in revised form 11 March 2021; Accepted 13 April 2021
Available online 22 April 2021

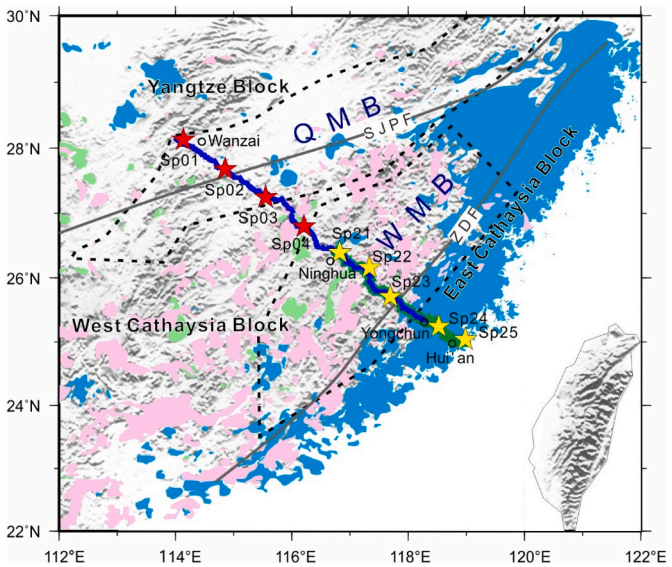

Fig. 1. Map showing the location of the deep seismic sounding profile and geological structure.
Red and yellow stars are artificial source points, while blue and green triangles show the deployment of short period seismic stations. Igneous rocks (after Zhou et al., 2006): light green areas represent Indosinian granites; pink areas show early Yanshanian granitoid-volcanic rocks; light blue areas covered by late Yanshanian granitoid-volcanic rocks. Faults: SJPF: Shaoxing-Jiangshan-Pingxiang fault; ZDF: Zhenghe-Dapu fault. Metallogenic Belt: QMB: Qinhang Metallogenic Belt; WMB: the Wuyishan Metallogenic Belt. (For interpretation of the references to colour in this figure legend, the reader is referred to the web version of this article.)

origin in deep mafic igneous protoliths in the middle-lower crust caused by underplating of basaltic magmas (Zhou et al., 2006). Therefore, the spatial and temporal distribution of Mesozoic granitoid-volcanic rocks in SE China occurred in changing tectonic environments in the course of different geodynamic processes.

Many geodynamic models have been proposed to interpret the mechanism of the Mesozoic granitoids and the mineral resource deposits in South China (Li and Li, 2007; Lin et al., 2018). Generally, these models can be classified into two groups: flat-slab subduction (Li and Li, 2007) and multi-terrane interaction (Lin et al., 2018). The crustal thickness, as well as the distribution of P wave velocity in the crust and uppermost mantle can provide tight constraints on the formation of granitoid rocks and evidence of deep geodynamic processes. In fact, several studies based on seismic tomography in SE China provide images of crustal and lithospheric structures at different scales. Receiver function results show that the crustal thickness from H-κ stacking method is about 38–46 km in the west of South China and about 26–34 km in the east of South China, with the Poisson's ratio between 0.20 and 0.31 (Ai et al., 2007; Li et al., 2013; Ye et al., 2013, 2014; Guo et al., 2019; Shen et al., 2019). The lithospheric thickness is also much greater in the west of South China (about 190 km) and much smaller in the east of South China (less than 100 km), even 60–70 km in the southeast coast of South China (Li et al., 2013; Ye et al., 2014; Lü et al., 2021). Surface wave tomography (Wang et al., 2015; Shen et al., 2016; Li et al., 2018; Li et al., 2020; Peng et al., 2020) results also reveal that the crustal and lithospheric structure present a significant difference in the west of South China and the east of South China. However, since the average resolution of the broad-band seismographs is greater than 10 km, the fine structure of the crust does not seem to be adequately resolved.

In contrast, Wide Angle Reflection and Refraction (WARR) profile can provide a detailed P wave velocity image of the crust and uppermost mantle. Several WARR profiles have been conducted in recent years (Deng et al., 2011; Zhang et al., 2013b; Li et al., 2015; Cai et al., 2016; Kuo et al., 2016). The results prove that the crustal thickness ranges from 35 km in the eastern Yangtze Block to 28 km in the Taiwan Strait, the average crustal velocity is about 6.2 km/s in the Cathaysia Block. These WARR profiles emphasize different crustal P-wave velocities in the east and west Cathaysia Block, with relatively high velocity in the middle-lower crust below East Cathaysia (Li et al., 2015; Cai et al., 2016; Kuo et al., 2016). However, these profiles focus mainly on East Cathaysia and the edge of West Cathaysia. In addition, WARR data on the structure of the crust in the Qinhang Metallogenic Belt (QMB) and the Wuyishan Metallogenic Belt (WMB) (Fig., 1) are essential for understanding the regional dynamics.

In order to investigate the area of Mesozoic granitoids and the mineral resources in SE China, we review previous WARR profile data from Ninghua to Hui'an that was later completed with a new WARR profile from Wanzai to Yongchun (Fig., 1). We use the 2D ray tracing method with RAYINVR inversion algorithm (Zelt and Smith, 1992) to model the crustal and uppermost mantle P-wave velocity structure of the QMB, WMB and East Cathaysia. Finally, we discuss the crustal and lithospheric thinning, crustal P-wave velocity characteristics, regional mineralization, and related tectonic evolution in SE China.

2. Tectonic setting

The Shaoxing-Jiangshan-Pingxiang fault (SJPF) divides the South China into the Yangtze Block to the northwest and the Cathaysia Block to the southeast. The Yangtze Block contains an Archean-Paleoproterozoic crystalline basement while the Cathaysia Block is divided into two zones, West Cathaysia and East Cathaysia (Xu et al., 2007; Lin et al., 2018). The West Cathaysia has a Precambrian basement and is affected by a major magmatic and metamorphic event during the Early Paleozoic, while the East Cathaysia consists of a series of metasedimentary and metaplutonic rocks (Xu et al., 2007).

Southeast China experienced multi-stage intracontinental orogeny since the Neoproterozoic, resulting in the 1300 km wide South China fold belt and widely distributed Mesozoic granitoids (Zhou et al., 2006; Li and Li, 2007; Wang et al., 2013). Two periods of tectono-magmatism are recognized since the Mesozoic in South China, the Indosinian (Triassic) magmatism and the Yanshanian (Jurassic-Cretaceous) magmatism. The Early Indosinian period is *syn*-collisional, and was formed in a compressional setting, while the Late Indosinian period is late-collisional, and was formed in a locally extensional environment. The Early Yanshanian granitoid-volcanic rocks are characteristic of rift-type intraplate magmatism, whereas the Late Yanshanian magmatism is likely active continental margin magmatism (Zhou et al., 2006).

The Qinhang Metallogenic Belt (QMB) and the Wuyishan Metallogenic Belt (WMB) are two important metallogenic belts in SE China (Fig., 1), which are rich in copper, tungsten, tin etc. These two metallogenic belts had experienced complex tectonism since the Neoproterozoic, but the primary mineral resources were formed during the Mesozoic period (Mao et al., 2011; Mao et al., 2014).

3. Wide-angle seismic data and phase analysis

3.1. Seismic data acquisition

In December 2018, the Institute of Geology and Geophysics, Chinese Academy of Sciences, with the support of the China Key National R&D Program, completed a NW-SE-trending WARR profile from Wanzai to Yongchun up to a total length of 530 km (Fig. 1). Four shots (red stars in Fig. 1) were fired along the profile at an interval of about 80–90 km. The explosive charge of each shot varied from 2000 kg to 2520 kg. Along the profile, 435 portable seismographs (blue triangles in Fig. 1) were deployed with an average interval of about 1.2 km. Previously, to study the deep tectonic structure of the SE margin in mainland China, a 270 km long WARR profile (Cai et al., 2016), from Ninghua to Hui'an, was conducted by the Earthquake Administration of Fujian Province, China

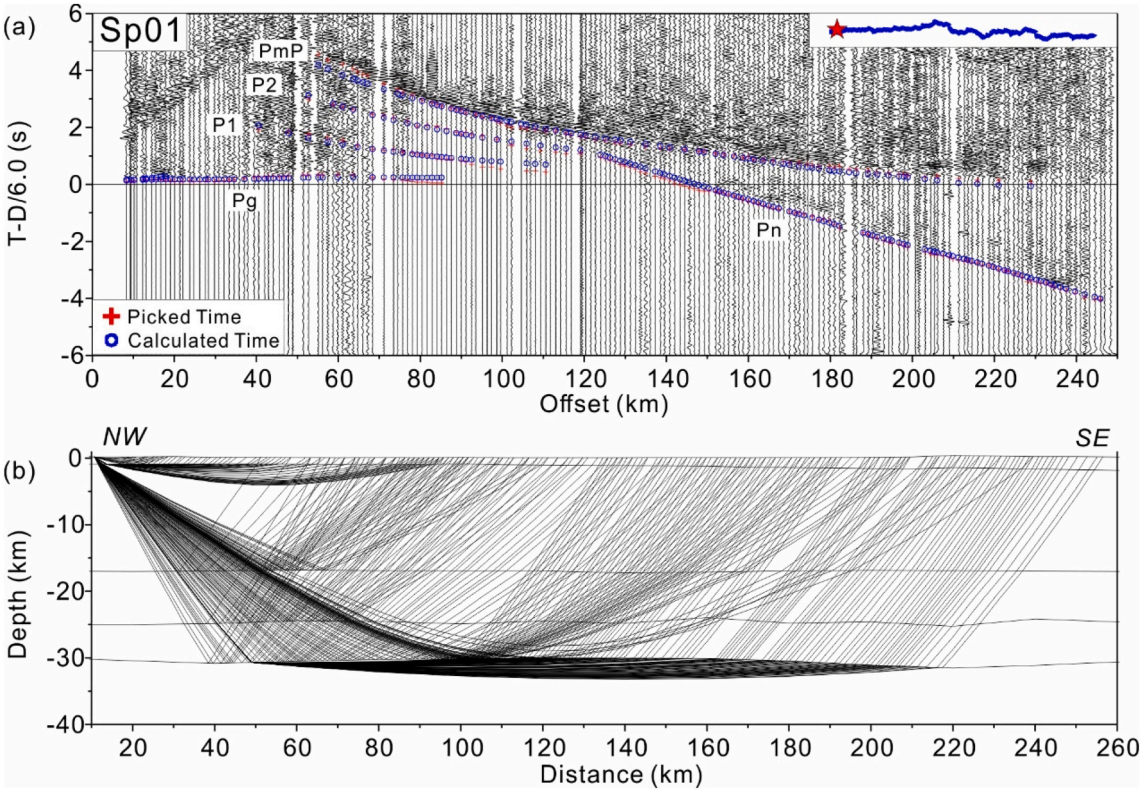

Fig. 2. (a) P-wave record section (on a reduced time scale with a reduction velocity of 6.0 km/s) corresponding to the shot point Sp01 and identified seismic phases. Red crosses and blue circles indicate picked times and calculated times, respectively Top right inset: the star indicates the location of the shot and the triangles represent seismographs. (b) Ray tracing diagram. (For interpretation of the references to colour in this figure legend, the reader is referred to the web version of this article.)

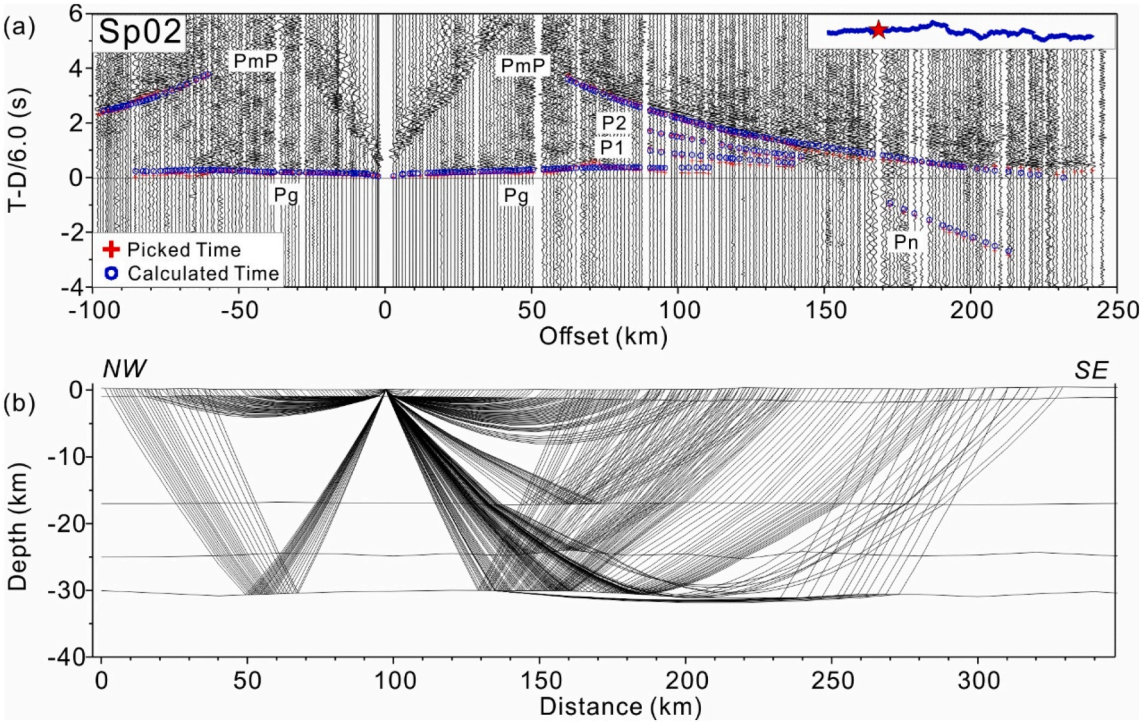

Fig. 3. Same as in Fig. 2 for shot point Sp02.

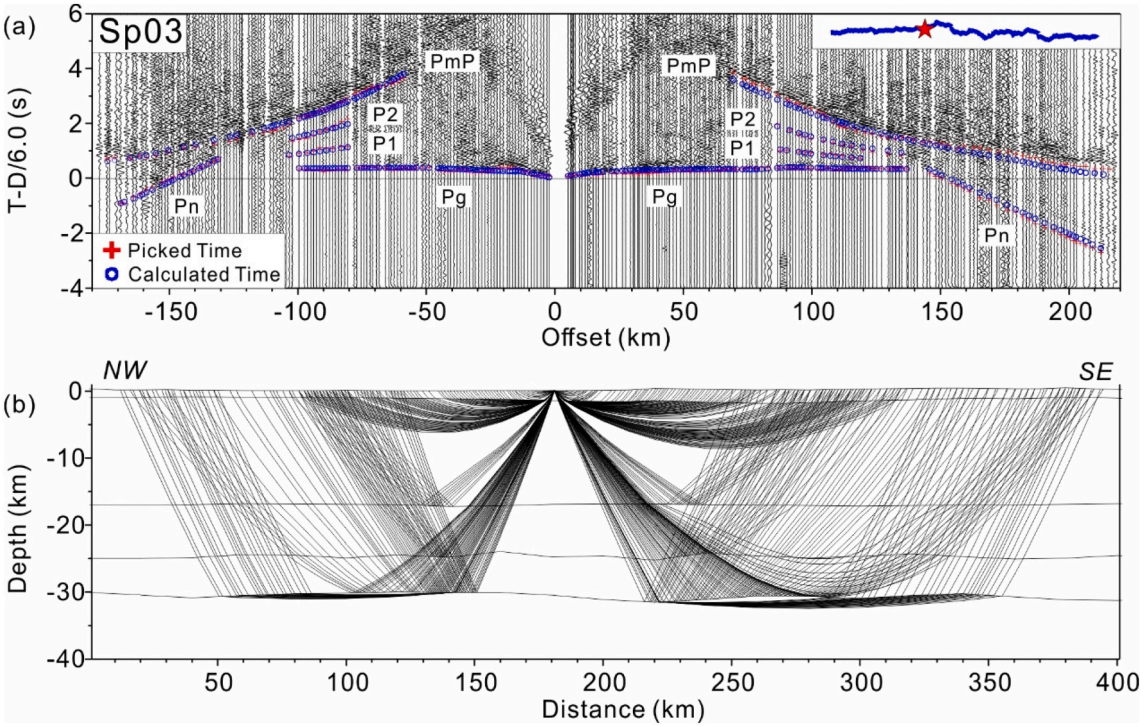

Fig. 4. Same as in Fig. 2 for shot point Sp03.

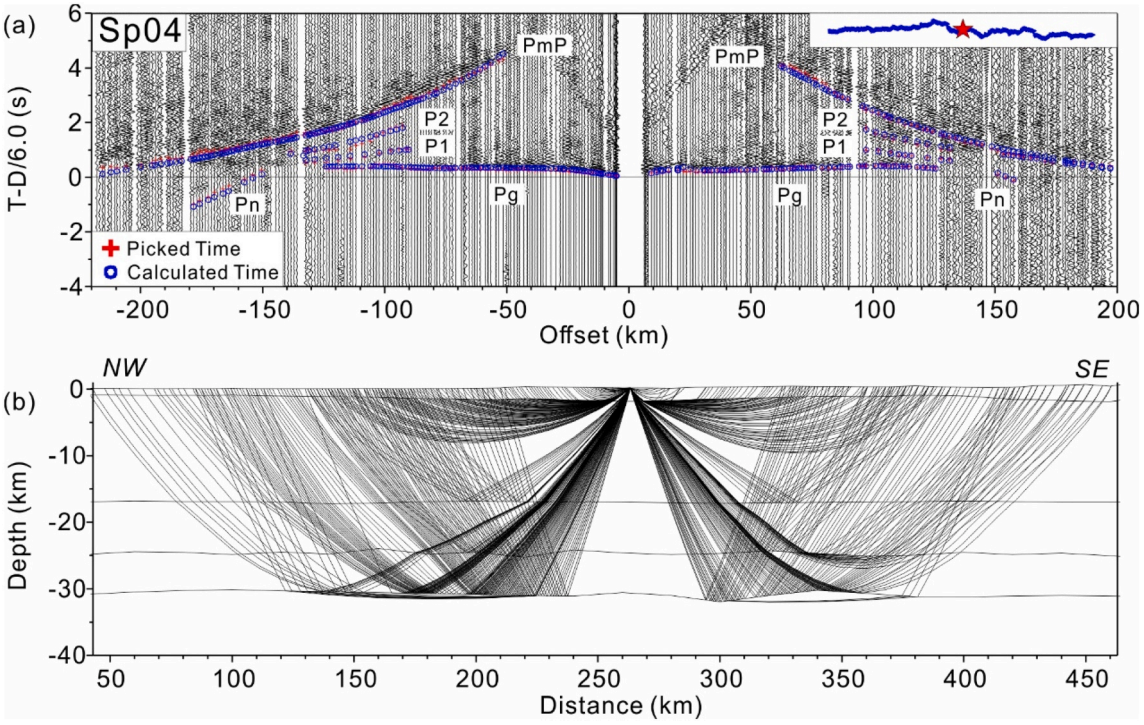

Fig. 5. Same as in Fig. 2 for shot point Sp04.

from June to August 2012. On that occasion, five shots (yellow stars in Fig. 1) were fired and 160 portable seismographs (green triangles in Fig. 1) were deployed along the profile, with shot points and receivers spaced 50 to 98 km and 1.5 to 2.0 km, respectively. These two WARR profiles have the same NW-SE direction and an overlap distance of about 195 km between Ninghua and Yongchun. In this paper, we combined these two profiles to obtain the crustal and uppermost mantle P wave velocity structure along the Wanzai-Hui'an transect, which covers approximately 620 km.

3.2. Seismic phases on the record sections

Travel times are picked on shot gathers using the interactive plotting and picking program ZPLOT. All record sections (Figs. 2–10; Fig. S1-S9)

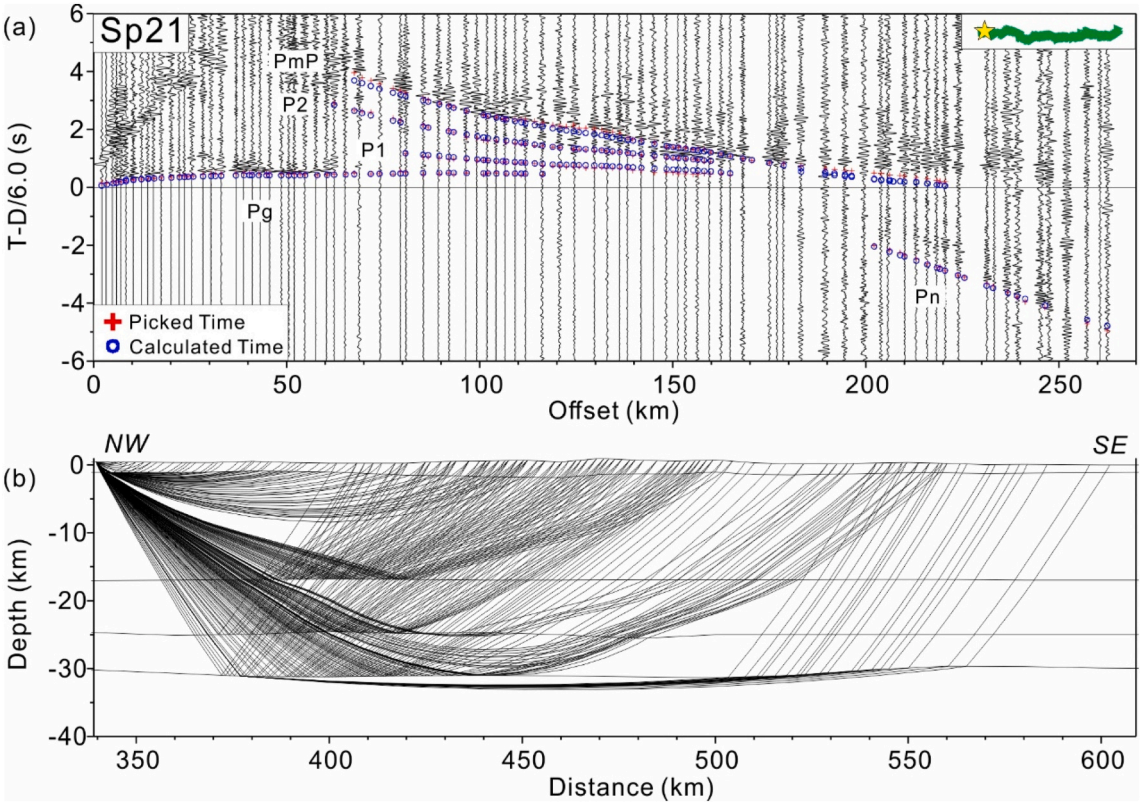

Fig. 6. Same as in Fig. 2 for shot point Sp21.

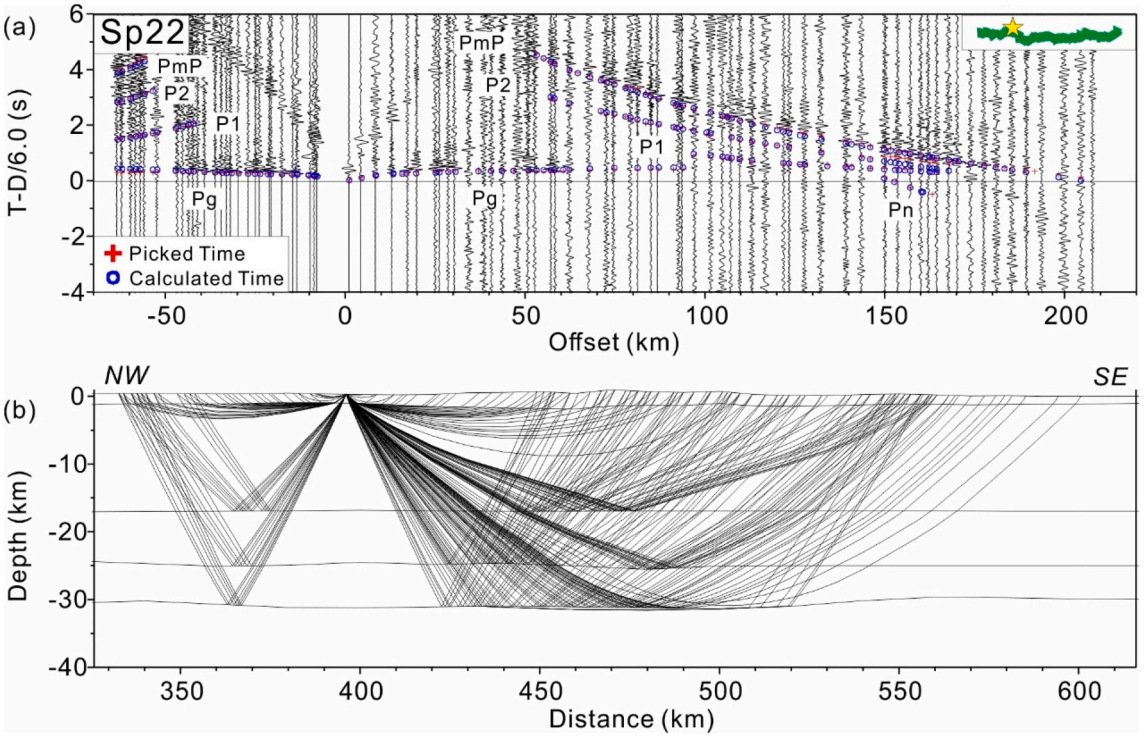

Fig. 7. Same as in Fig. 2 for shot point Sp22.

are filtered by a 2–10 Hz band-pass filter and travel time is reduced by a velocity of 6.0 km/s, in order to emphasize the detail of the crust. Several crustal and uppermost mantle seismic phases were recorded, including refracted phase in the upper crust (Pg), reflected phases in the crystalline crust (P1, P2), reflected phases from the Moho (PmP) and refractions in uppermost mantle (Pn).

The refracted phase (Pg) can be picked at offsets of about 0–130 km, and has an apparent velocity between 5.8 and 6.1 km/s. The reduced

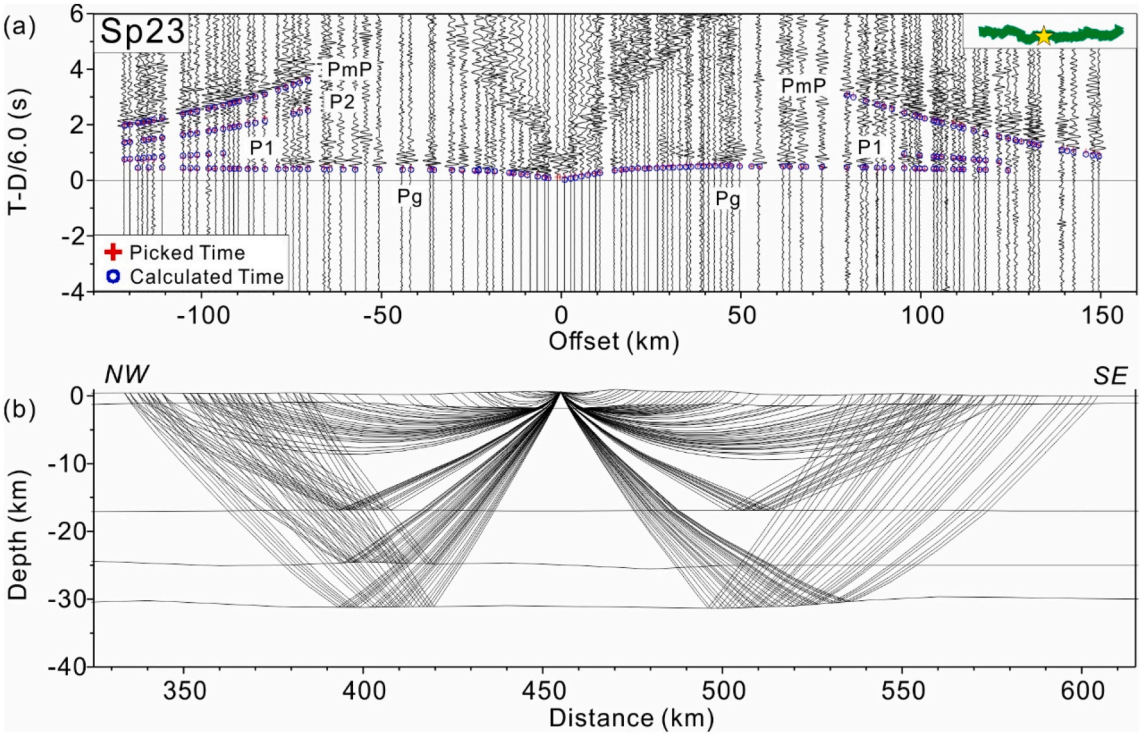

Fig. 8. Same as in Fig. 2 for shot point Sp23.

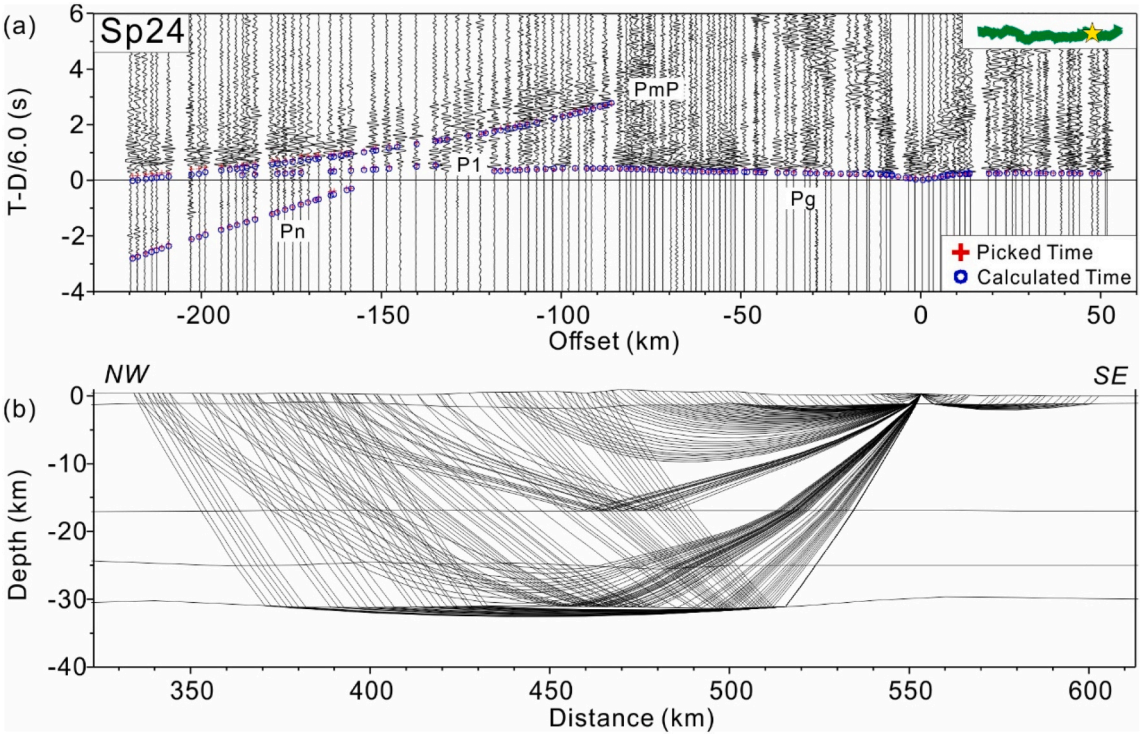

Fig. 9. Same as in Fig. 2 for shot point Sp24.

time of Pg phase ranges from 0.1 to 0.4 s, indicating a relatively thin sedimentary cover in SE China. Intracrustal reflected phases (P1, P2) can be recognized at the offsets of 50–190 km, with two group of phases P1 and P2 can be picked beneath Yangtze and West Cathaysia, while only one group of P1 can be recognized beneath East Cathaysia. The intracrustal reflected phases are distinctly weaker than PmP, implying a relatively low impedance contrast of P wave. The PmP phase is clearly recorded at the offset of 50–240 km and generally show great amplitude in all record sections. PmP arrivals on the record section of shot point Sp24 and Sp25 are earlier than other record sections, revealing that the Moho depth is shallower beneath East Cathaysia. The upper mantle refracted phase Pn appears at offset of 120–270 km, with an apparent

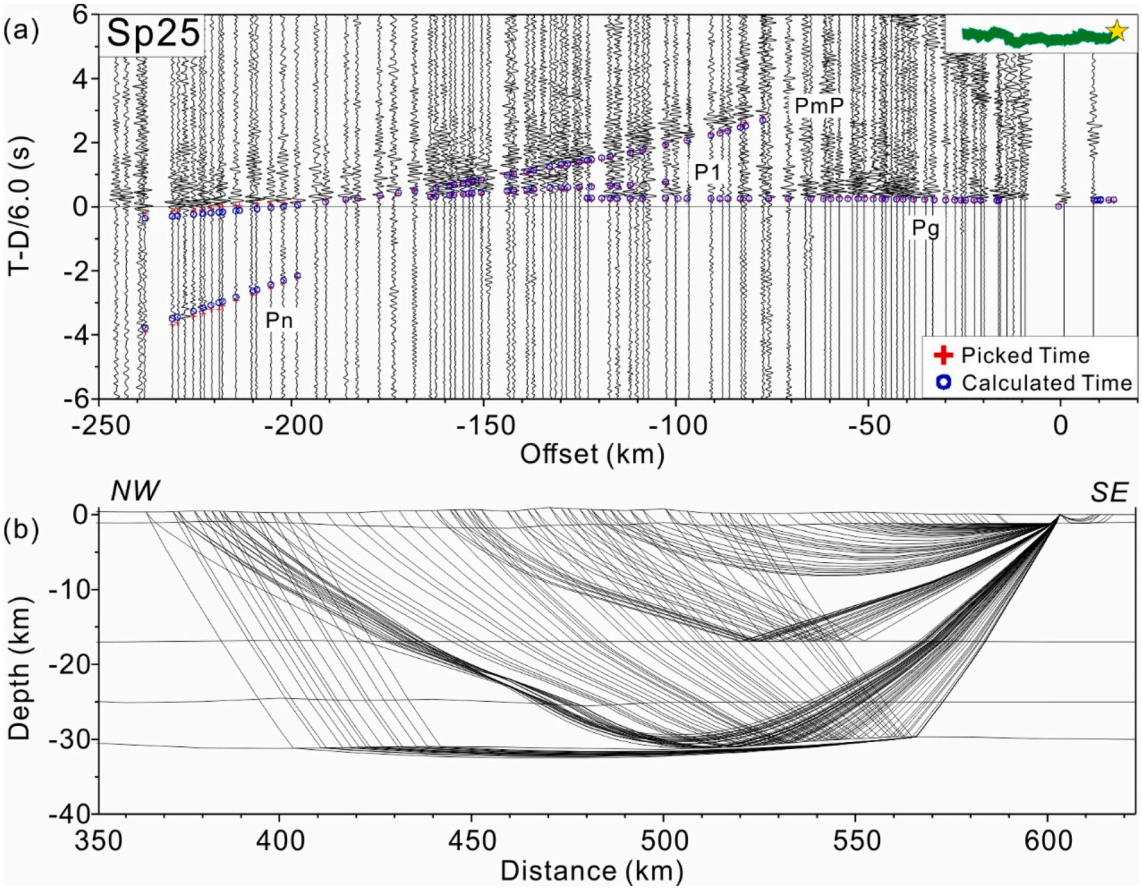

Fig. 10. Same as in Fig. 2 for shot point Sp25.

Table 1
Ray tracing details for individual seismic phases.

Seismic phase	Total number of picks	Number of modelled picks	The percentage of traced picks	RMS (s)	χ^2
Pg	869	854	98.3%	0.066	1.756
P1	229	229	100.0%	0.084	0.713
P2	200	200	100.0%	0.092	0.856
PmP	767	755	98.4%	0.132	1.757
Pn	240	225	93.7%	0.132	1.749

velocity of 8.0–8.1 km/s.

3.3. Seismic data processing

First arrivals of Pg in WARR record sections have the highest signal to noise ratio, which can be used to constrain an accurate upper crustal velocity model. In this paper, the 2D finite-difference inversion method (Vidale, 1988, 1990; Hole, 1992) was used to invert for the upper crustal structure. This method is much faster than two-point ray tracing method and more robust in highly heterogeneous media. A total of 869 Pg travel-time picks was used to invert for the upper crust velocity. The grid size in the upper crust model is 0.5 × 0.5 km, the back-projection method was applied to invert for the model, with a grid-spacing of 1.0 × 1.0 km. The final model was calculated after 30 iterations, with the root-mean-square (RMS) travel time residual reducing from 0.12 s to 0.02 s.

Also, we use the RAYINVR 2D ray-tracing and inversion algorithm (Zelt and Smith, 1992) to model the structure of the crust and uppermost mantle. Firstly, we use the 1D travel time fitting method, which is a trial and error method, and the finite-difference inversion method to construct an initial laterally-varying 2D velocity model (Lin et al., 2020). Then, all recognized phases (Pg, P1, P2, PmP and Pn) were used to determine the final model in a layer-by-layer forward modeling technique and keeping the shallow nodes constant when modeling the deep layers. The velocity model is iteratively modified several times until the RMS (root-mean-square) travel time residual approaches the data uncertainty, which is about 0.05 s for Pg phase and 0.1 s for other phases. Moreover, the normalized chi square value (χ2) is close to one and the highest possible number of picks has been used (Table 1). Travel time fitting of all these 9 shots (Fig. 11a) reveals that the fitting is relatively good and the ray coverage (Fig. 11b) is dense and evenly distributed along the whole profile.

4. Seismic velocity structure of the crust and uppermost mantle

The final 2D velocity model (Fig. 12a) presents laterally varying of P-wave velocity in the crust and a relatively slight smooth variation of the Moho depth and uppermost mantle. The crustal thickness is 30–32 km beneath the Yangtze and west Cathaysia, and slightly shallower (29–30 km) beneath east Cathaysia. The Bouguer gravity anomaly (Fig. 12b) along our profile also shows a gradual increase in East Cathaysia, which is conforming to the Moho depth (Fig. 12a). The average crustal velocity is 6.14–6.18 km/s beneath the Yangtze and West Cathaysia and 6.23–6.25 km/s beneath East Cathaysia.

The upper crust reveals as a heterogeneous structure along the profile. The thickness of the sedimentary cover is relatively thin (1.0–3.0 km), taking the contour line of 5.8 km/s as the base of the sedimentary layer. Nevertheless, it is thicker at distance of 300–500 km than in other parts of the transects. The P-wave velocity of the upper crust is 4.5–6.2 km/s, with 4.5–5.8 km/s in the sedimentary layer. The C1 interface occurs at a depth of about 17 km. The P-wave velocity shows an abrupt

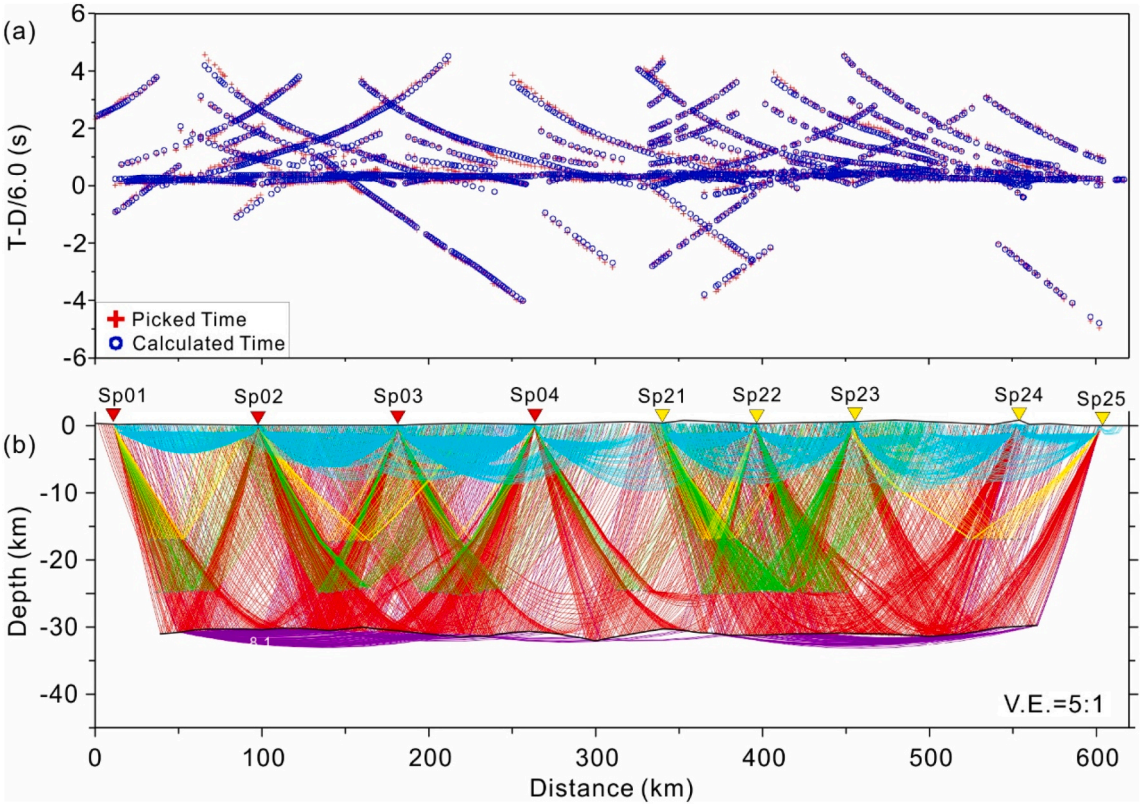

Fig. 11. Travel time fitting and ray coverage of all shots. (a) Red crosses and blue circles indicate the picked time and calculated time respectively. (b) Cyan, yellow, green, red and purple rays represent Pg, P1, P2, PmP and Pn respectively. (For interpretation of the references to colour in this figure legend, the reader is referred to the web version of this article.)

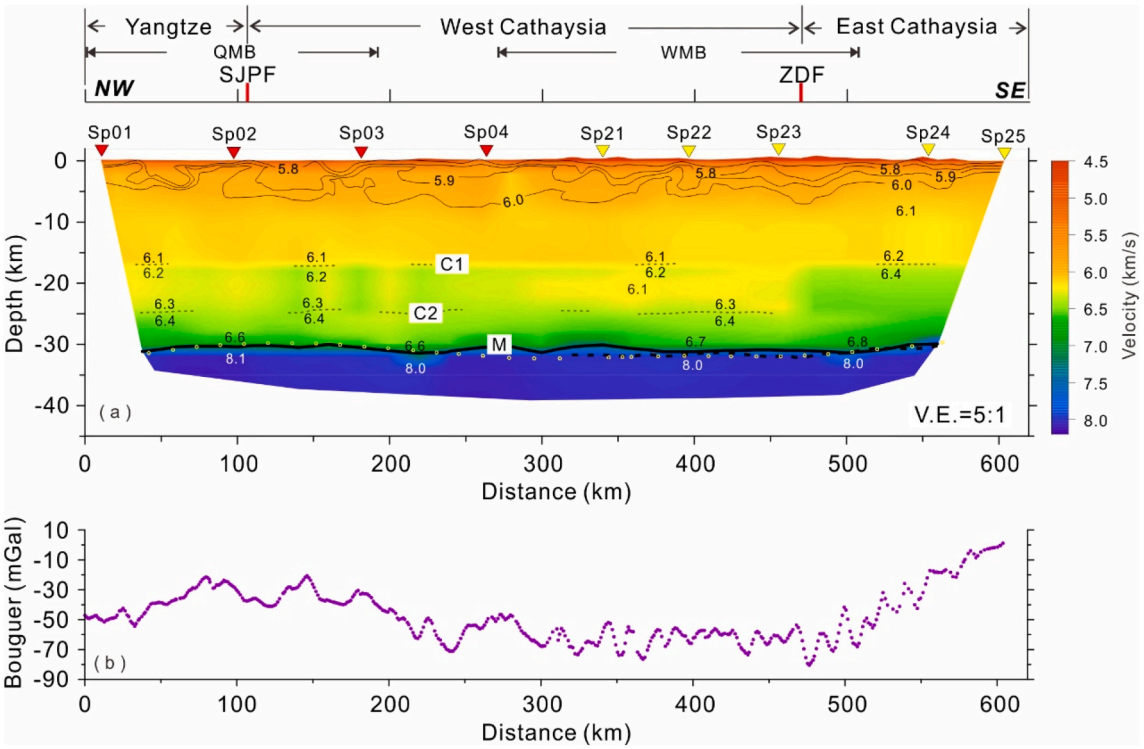

Fig. 12. (a) Two-dimensional crustal P-wave velocity model along the Wanzai-Hui'an profile. The top panel shows the tectonic units and faults which are crossed by the profile: SJPF, Shaoxing-Jiangshan-Pingxiang fault; ZDF: Zhenghe-Dapu fault. Metallogenic Belt: QMB: Qinhang Metallogenic Belt; WMB: the Wuyishan Metallogenic Belt. C1, C2 and M indicate C1, C2 interfaces and Moho discontinuity. The contour lines less than 6.1 km/s in the upper crust are derived from the 2D finite-difference result (Lin et al., 2020). (b) Bouguer gravity anomaly along the Wanzai-Hui'an profile.

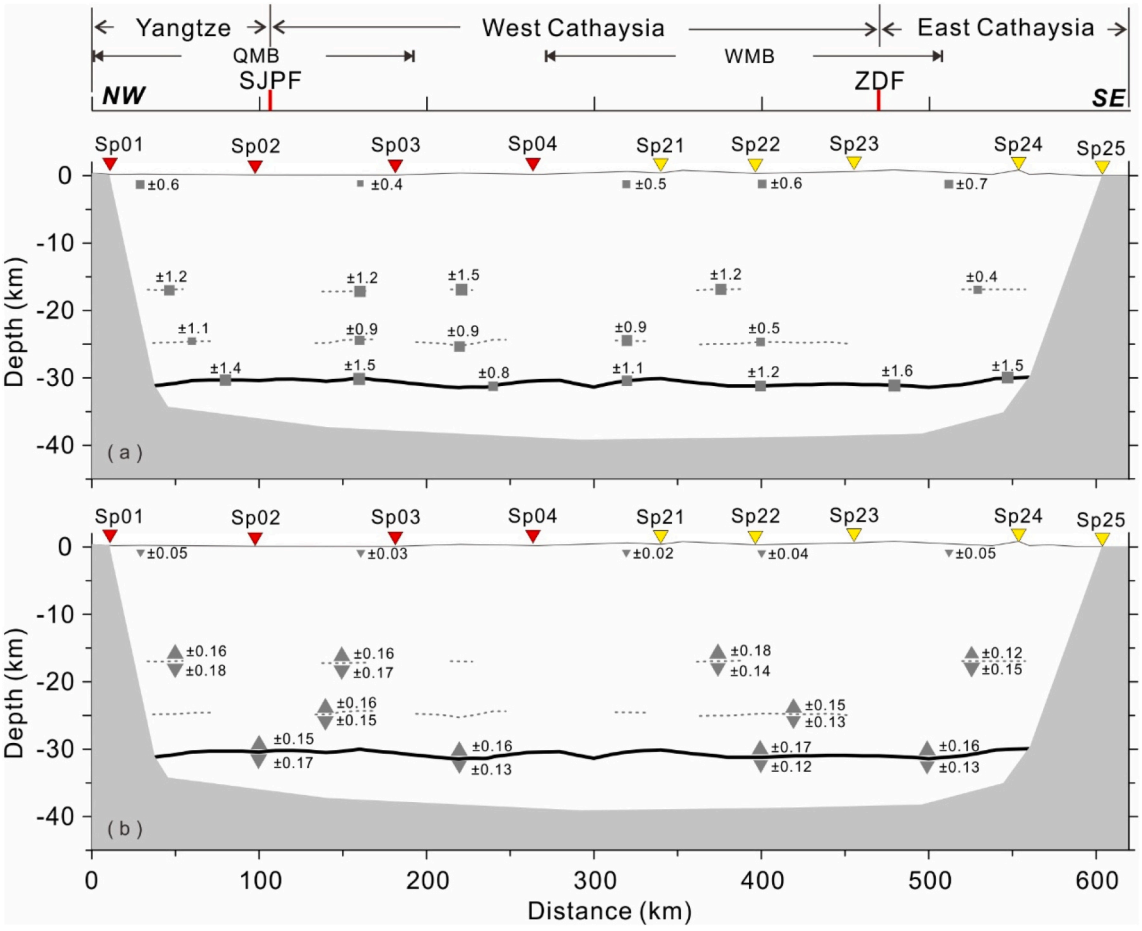

Fig. 13. Resolution test on the final 2-D velocity model. (a) Uncertainties in the layer boundaries in km. (b) Uncertainties of the seismic velocities in km/s. The size of the symbols is relative to the absolute values. The dashed lines indicate the reflections within the crust, while the thick black line represents the Moho.

change beneath the SJPF and ZDF fault, so it can be affected by these two faults.

The middle-lower crust in East Cathaysia shows higher P-wave velocity (6.4–6.8 km/s) than in the Yangtze and west Cathaysia (6.2–6.7 km/s). The C2 interface that reaches a depth of 25 km separates the middle crust from the lower crust, although this limit remains undefined beneath East Cathaysia. The velocity at 19–23 km depth below the WMB is relatively lower (6.1 km/s) than in any other zone at the same depth. The velocity of the uppermost mantle is 8.0–8.1 km/s, without distinct difference throughout the entire profile (Fig. 12a).

5. Resolution tests

We use a single parameter test (Nielsen and Thybo, 2009; Zelt, 1999) to analyze the spatial resolution of the model. A single parameter (a single depth or velocity node) was tested at a time. Then, the maximum possible changes of the depth nodes or the velocity nodes can be measured without unacceptable ray coverage, RMS misfit and chi square values. According to our analysis, the upper crustal boundaries, middle-lower crustal boundaries and the Moho are well constrained with a maximum uncertainty of ±0.7 km, ±1.5 km and ± 1.6 km respectively (Fig. 13a). The uncertainty of the velocity nodes are between ±0.02 km/s and ± 0.05 km/s in the upper crust, ±0.12 km/s and ± 0.17 km/s in the middle-lower crust (Fig. 13b), which are well defined and can be ascribed to the dense ray coverage of the model.

6. Discussion

6.1. Comparison with other results

We compare our result with Cai et al.'s (2016) WARR profile, which runs from Ninghua to Hui'an (Fig. 1). The thick dashed line in Fig. 12a is the Moho depth of Cai et al.'s result. The Moho has the same pattern at the distance of 320–560 km with our Moho depth, except a little small-scale discrepancy at the distance of 320–360, due to the different ray coverage of the new Sp04 record section. Zhang et al. (2021) got a three-dimensional Moho depth model based on receiver function method, and the Moho depth (yellow circles in Fig. 12a) shows a good agreement with our result, which reveals the reliability of our model.

We also compare our result with other seismic profiles or arrays, which are in the vicinity of our profile. Wei et al. (2016) and Han et al. (2019) got the average crustal thickness is about 30.43 km in Cathaysia Block and of 31.2 km in the central part of Cathaysia Block. The Moho depth from Li et al. (2015) also shows the same characteristic with our result, 30–33 km beneath Cathaysia Block and a relatively low velocity layer at the depth of 22 km beneath the east part of West Cathaysia. Another WARR profile (Zhang and Wang, 2007; Zhang et al., 2013b) in the SW direction of our profile shows that the Moho is about 30–34 km beneath the Yangtze and Cathaysia Block and a low velocity layer at the depth of 15–20 km. The middle and lower crust present relatively high velocity beneath East Cathaysia in Li et al.'s (2015), Cai et al.'s (2016) and our result, which is about 0.2 km/s higher than West Cathaysia. Both the WARR and Receiver function evidence reveal that the crustal thickness in east Yangtze and Cathaysia Block varies between 29 and 35

km and is gradually less from inland to shore.

6.2. Lithospheric and crustal thinning

Lithospheric and the crustal thinning may provide some information about the deep geodynamic processes. Previous geophysical results demonstrate that the lithospheric thickness in eastern China has evolved since the Mesozoic (Chen et al., 2008; Zhu et al., 2012; Deng and Levandowski, 2018). P and S wave receiver functions show that the lithospheric thickness beneath the Cathaysia Block is less than 100 km (Zhang et al., 2018), being only 60–70 km in East Cathaysia (Li et al., 2013; Ye et al., 2014). However, the lithosphere is thicker (approximately 190 km) in the west of the Yangtze Craton (Zhang et al., 2018). Likewise, the Moho depth also varies from 45 to 50 km in the West Yangtze Craton to about 30 km in the Cathaysia Block (Li et al., 2013; Ye et al., 2014), showing the same variation features with the lithosphere thickness. In addition, Rayleigh wave tomography (Wang et al., 2015; Shan et al., 2017) and the joint inversion of receiver functions and surface wave dispersion (Li et al., 2018; Deng et al., 2019) also prove that the crust and lithosphere are significantly thinned in eastern China.

Geochemical results constrained a thick lithosphere (110–230 km) below South China in the Paleozoic period (Zheng et al., 2015) and a thinner lithosphere (less than 80 km) during the late Mesozoic time (Liu et al., 2012). Similarly, North China came to had an ancient thick lithosphere (about 200 km) in the Archean period, characteristic of a craton, and then underwent extensive modification during the late Mesozoic period (Zhu et al., 2011, 2012). Thus, both the eastern part of south China and north China craton experienced significant destruction and thinning of the lithosphere. Meanwhile, crustal thickness in eastern China was also reduced to about 30 km (Li et al., 2013; Jia et al., 2014; Tian et al., 2014; Ye et al., 2014; Li et al., 2015; Cai et al., 2016), relative to the global average crustal thickness of shields and platforms, which is 41.5 km (Christensen and Mooney, 1995).

6.3. Main tectonic boundaries

The Shaoxing-Jiangshan-Pingxiang Fault (SJPF) is considered as the boundary between the Yangtze and Cathaysia Block (Li, 1992; Zhang et al., 2005). Our results show distinct heterogeneity in the upper crust beneath the SJPF, but no significant changes in the middle and lower crust, which can be attributed to insufficient ray coverage of the Yangtze Block.

The Zhenghe-Dapu Fault (ZDF) divides the Cathaysia into two parts: the western part and eastern part (Xu et al., 2007; Li et al., 2015; Cai et al., 2016). The discrepancy of middle and lower crust on the east and west side of ZDF fault provides evidence that the ZDF fault may probably extend into the deep crust. Recently, Lin et al.'s (2018) evidence from Zircon U-Pb ages, Hf data, and structural data proposed that the boundary between the west and east Cathaysia is not the ZDF, but the northwest Fujian fault that is located about 50 km northwest of ZDF. Considering the obvious difference of velocity in the middle and lower crust, we speculate the deep boundary between the west and east Cathaysia is the ZDF.

6.4. Tectonic evolution in SE China

The velocity model (Fig. 12a) is characterized in the middle-lower crust by the relatively low velocity zone (6.1 km/s) below the WMB and the high velocity zone (6.4–6.8 km/s) below the east Cathaysia. Based on the regional tectonic activity, we believe that the low velocity zone below the WMB may be ascribed to the ductile shear zones (Zhang and Wang, 2007), which are related to the delamination during the Late-Caledonian (Silurian) period and the lithospheric extension during Yanshanian (Jurassic-Cretaceous) period. The relatively high velocity zone in the middle-lower crust in East Cathaysia may be attributed to the slab rollback of the Paleo-Pacific plate (Zhao et al., 2013; Li et al., 2014; Li et al., 2017), which provides more mafic material to the middle-lower crust. Furthermore, the late Yanshanian (Cretaceous) underplating of East Cathaysia may increase the middle-lower crustal velocity and result in the widely distributed Cretaceous volcanic rocks in East Cathaysia (Xu et al., 2007; Shu et al., 2009; Zhang et al., 2009; Lin et al., 2018).

According to previous geological, geophysical studies (Zhou et al.,

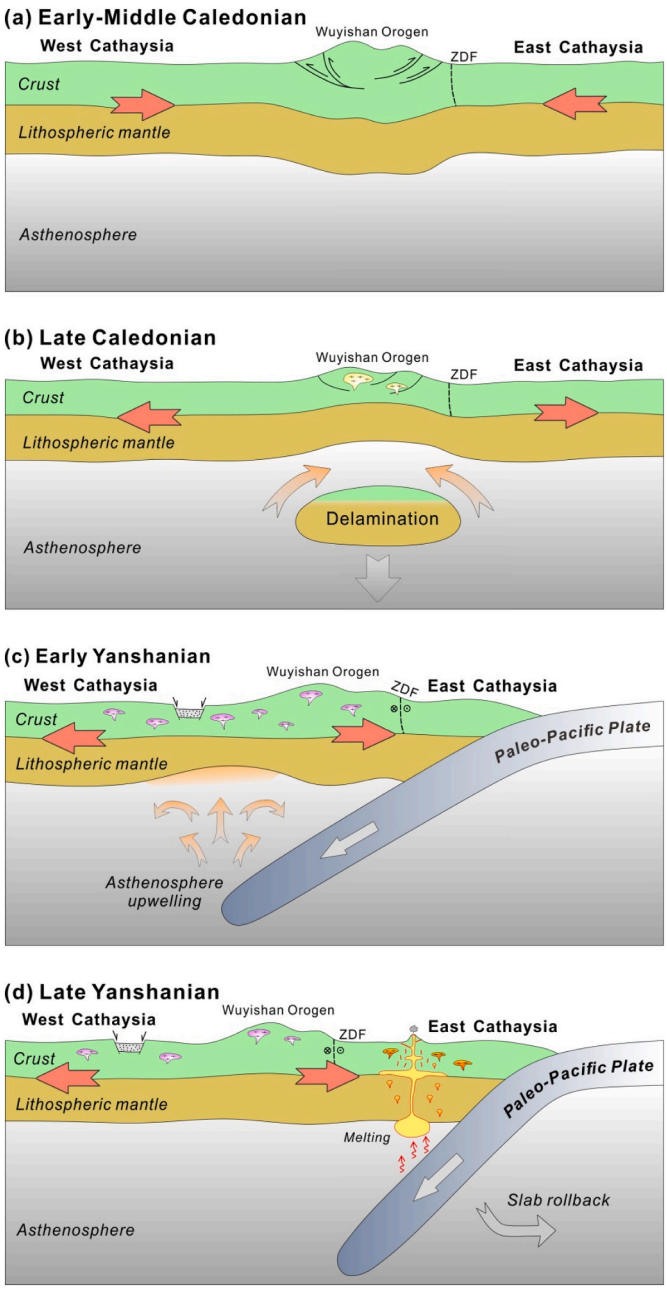

Fig. 14. Schematic cartoon illustrating the tectonic evolution of the Cathaysia in SE China. (a) During the early-middle Caledonian (Ordovician), the crust and lithospheric mantle were thickened due to the intracontinental orogeny of the south China block. (b) During the late Caledonian (Silurian), in response to the post-collisional extension, the lower crust and lithospheric mantle collapsed. (c) During the early Yanshanian (Jurassic), the paleo-Pacific plate started its subduction and led to the asthenosphere upwelling, and then the back-arc extension resulted in the crustal material melting, which provided the source to the widely distributed early Yanshanian (Jurassic) granite in west Cathaysia. (d) During the late Yanshanian (Cretaceous), continuous extension resulted in the slab rollback of the paleo-Pacific plate, and the dip of the slab increased, and extensive melting and magma underplating caused the late Yanshanian (Cretaceous) granite and volcanic rocks in east Cathaysia.

2006; Shu, 2012; Wang et al., 2013; Zhang et al., 2013a; Shu et al., 2015) and the crustal P-wave velocity structure shown in this paper, we can describe a larger picture in relation to the velocity structure and the tectonic evolution in SE China on a geological time scale (Fig. 14). Four stages can be distinguished, namely: Early-Middle Caledonian (Ordovician) period (Fig. 14a), the Late Caledonian (Silurian) period (Fig. 14b), the early Yanshanian (Jurassic) period (Fig. 14c) and the late Yanshanian (Cretaceous) period (Fig. 14d). First, the Caledonian Orogeny between West Cathaysia and East Cathaysia resulted in the crustal thickening (Wang et al., 2013). Second, after post-orogenic extension, the lower crust and lithosphere collapsed (Wang et al., 2013). Third, the Paleo-Pacific plate started to subduct underneath the Eurasian plate. Accompanying this subduction, the lithospheric mantle was heated up and the asthenospheric upwelling made the extensional tectonic framework continue (Zhou and Li, 2000; He and Xu, 2012; Liu et al., 2015). Under an extensional tectonic regime, the crust and lithosphere in SE China were thinned distinctly. Finally, due to the ongoing extension, the dip angle of the subduction increased as a result of slab rollback, and the subducted slab dehydration brought about more adakitic and felsic melts, resulting in extensive underplating in the lower crust (Zhang et al., 2009; Zhao et al., 2013; Li et al., 2014; Li et al., 2017). We believe that the subduction of the Paleo-Pacific plate and the slab rollback provide the environmental conditions for the emergence of the Mesozoic granitoids and the mineral resources in SE China.

7. Conclusions

Based on the interpretation of the 620 km long wide-angle seismic profile between Wanzai and Hui'an across the Yangtze Block and Cathaysia, we propose the following conclusions:

(1) The crustal thickness in East Yangtze and Cathaysia is about 29–32 km and shows a gradual thinning pattern from inland to shore.
(2) Our crustal velocity model shows that the SJPF fault is the boundary between the Yangtze and West Cathaysia and the ZDF fault is the boundary between West and East Cathaysia.
(3) There is a low velocity layer at a depth of about 20 km below the WMB. We speculate that it can be due to the existence of the ductile shear zones, as the consequence of a delamination process during the Caledonian (Ordovician- Silurian) orogeny and the lithospheric extension during the Yanshanian (Jurassic- Cretaceous) period.
(4) The crust in East Yangtze and the Cathaysia has been thinned significantly, and the seismic velocity in the middle-lower crust is higher in East Cathaysia, which can be attributed to the underplating related to the slab rollback of the Paleo-Pacific plate during the late Yanshanian (Cretaceous) period.

Declaration of Competing Interest

We declare that this paper has not been submitted elsewhere. There are no conflicts of interest.

Acknowledgements

We would like to thank Geophysical Exploration Center of the China Earthquake Administration for providing us with the seismic fieldwork. Special thanks to two anonymous reviewers who provided constructive review comments. We would also like to thank Prof. Laicheng Miao, Prof. Jiayong Yan and Dr. Yunhao Wei for their helpful discussions. We appreciate the help of Dr. Chenglong Wu in making the cartoon figures. This study was funded by the National Key Research and Development Project of China (2016YFC0600201 and 2018YFC1503204) and the National Natural Science Foundation of China (41790461, 41774097 and 41774100).

Appendix A. Supplementary data

Supplementary data to this article can be found online at https://doi.org/10.1016/j.tecto.2021.228874.

References

Ai, Y., Chen, Q., Zeng, F., Hong, X., Ye, W., 2007. The crust and upper mantle structure beneath southeastern China. Earth Planet. Sci. Lett. 260, 549–563.
Cai, H., Jin, X., Wang, S., Li, P., Chen, W., 2016. The crust structure and velocity structure characteristics beneath Ninghua-Datian-Hui'an. Chin. J. Geophys. 59 (1), 157–168 (in Chinese).
Chen, L., Tao, W., Zhao, L., Zheng, T., 2008. Distinct lateral variation of lithospheric thickness in the northeastern North China craton. Earth Planet. Sci. Lett. 267 (1–2), 56–68.
Christensen, N.I., Mooney, W.D., 1995. Seismic velocity structure and composition of the continental crust: a global view. J. Geophys. Res. 100 (B7), 9761–9788.
Deng, Y., Levandowski, W., 2018. Lithospheric alteration, intraplate crustal deformation, and topography in eastern China. Tectonics 37, 4120–4134.
Deng, Y., Lin, S., Fan, W., Liu, J., 2011. Crustal structure beneath South China revealed by deep seismic sounding and its dynamics implications. Chin. J. Geophys. 54 (10), 2450–2574 (in Chinese).
Deng, Y., Li, J., Peng, T., Ma, Q., Song, X., Sun, X., Shen, Y., Fan, W., 2019. Lithospheric structure in the Cathaysia block (South China) and its implication for the late Mesozoic magmatism. Phys. Earth Planet. Inter. 291, 24–34.
Guo, L., Gao, R., Shi, L., Huang, Z., Ma, Y., 2019. Crustal thickness and Poisson's ratios of South China revealed from joint inversion of receiver function and gravity data. Earth Planet. Sci. Lett. 510, 142–152.
Han, R., Li, Q., Xu, Y., Zhang, H., Chen, H., Lang, C., Wu, Q., Wang, X., 2019. Deep structure background and Poisson's ratio beneath the intersection zone of Nanling and Wuyi. Chin. J. Geophys. 62 (7), 2477–2489 (in Chinese).
He, Z., Xu, X., 2012. Petrogenesis of the late Yanshanian mantle-derived intrusions in southeastern China: Response to the geodynamics of paleo-Pacific plate subduction. Chem. Geol. 328, 208–221.
Hole, J., 1992. Nonlinear high-resolution three-dimensional seismic travel time tomography. J. Geophys. Res. 97, 6553–6562.
Jia, S., Wang, F., Tian, X., Duan, Y., Zhang, J., Liu, B., Lin, J., 2014. Crustal structure and tectonic study of North China Craton from a long deep seismic sounding profile. Tectonophysics 627, 48–56.
Kuo, Y., Wang, C., Hao, K., Jin, X., Cai, H., Lin, J., Wu, F., Yen, H., Huang, B., Liang, W., Okaya, D., Brown, L., 2016. Crustal structures from the Wuyi-Yunkai orogen to the Taiwan orogen: the onshore-offshore wide-angle seismic experiments of the TAIGER and ATSEE projects. Tectonophysics 692, 164–180.
Li, H., Song, X., Lü, Q., Yang, X., Deng, Y., Ouyang, L., Li, J., Li, X., Jiang, G., 2018. Seismic imaging of lithosphere structure and upper mantle deformation beneath east-Central China and their tectonic implications. J. Geophys. Res. Solid Earth 123, 2856–2870.
Li, J., 1992. Study on Structure and Evolution of Oceanic-Continental Lithosphere in Southeast China. Press of China, Beijing, Sci. and Technol.
Li, J., Zhang, Y., Dong, S., Johnston, S., 2014. Cretaceous tectonic evolution of South China: a preliminary synthesis. Earth Sci. Rev. 134, 98–136.
Li, J., Sun, X., Wang, S., He, L., Fan, A., Zhang, P., 2020. Crustal shear wave velocity structure near the Jiujishan area from seismic ambient noise tomography: Implications for tectonic evolution in South China. Chin. J. Geophys. 63 (1), 184–195 (in Chinese).
Li, P., Jin, X., Wang, S., Cai, H., 2015. Crustal velocity structure of the Shaowu-Nanping-Pingtan transect through Fujian from deep seismic sounding-tectonic implications. Sci. China: Earth Sci. (in Chinese) 45, 1757–1767.
Li, Q., Gao, R., Wu, F., Guan, Y., Ye, Z., Liu, Q., Hao, K., He, R., Li, W., Shen, X., 2013. Seismic structure in the southeastern China using teleseismic receiver functions. Tectonophysics 606, 24–35.
Li, S., Zang, Y., Wang, P., Suo, Y., Li, X., Liu, X., Zhou, Z., Liu, X., Wang, Q., 2017. Mesozoic tectonic transition in South China and initiation of Paleo-Pacific subduction. Earth Sci. Front. (in Chinese) 24 (4), 213–225.
Li, Z., Li, X., 2007. Formation of the 1300-km-wide intracontinental orogen and postorogenic magmatic province in Mesozoic South China: a flat-slab subduction model. Geology 35 (2), 179–182.
Lin, J., Tang, G., Xu, T., Cai, H., Lü, Q., Bai, Z., Deng, Y., Huang, M., Jin, X., 2020. P-wave velocity structure in upper crust and crystalline basement of the Qinhang and Wuyishan Metallogenic belt: constraint from the Wanzai-Hui'an deep seismic sounding profile. *Chinese J. Geophys.* (in Chinese) 63 (12). https://doi.org/10.6038/cjg2020O0158.
Lin, S., Xing, G., Davis, D., Yin, C., Wu, M., Li, L., Jiang, Y., Chen, Z., 2018. Appalachian-style multi-terrane Wilson cycle model for the assembly of South China. Geology 46 (4), 319–322.
Liu, C., Liu, Z., Wu, F., Chu, Z., 2012. Mesozoic accretion of juvenile sub-continental lithospheric mantle beneath South China and its implications: geochemical and re-Os isotopic results from Ningyuan mantle xenoliths. Chem. Geol. 291, 186–198.
Liu, L., Xu, X., Xia, Y., 2015. Asynchronizing paleo-Pacific slab rollback beneath SE China: Insights from the episodic late Mesozoic volcanism. Gondwana Res. 37, 397–407.
Lü, Q., Wang, G., Zhang, K., Liu, Z., Yan, J., Shi, D., Han, J., Gong, X., 2021. The lithospheric architecture of the Lower Yangtze Metallogenic Belt, East China:

insights into an extensive Fe–Cu mineral system. Ore Geol. Rev. 132 https://doi.org/10.1016/j.oregeorev.2021.103989.
Mao, J., Chen, M., Yuan, S., Guo, C., 2011. Geological characteristics of the Qinhang (or Shihang) metallogenic belt in South China and spatial-temporal distribution regularity of mineral desposits. Atca Seismol. Sinica (in Chinese) 85 (5), 636–658.
Mao, J., Li, Z., Ye, H., 2014. Mesozoic tectono-magmatic activities in South China: Retrospect and prospect. Sci. China Earth Sci. 44 (12), 2593–2617 (in Chinese).
Nielsen, C., Thybo, H., 2009. No Moho uplift below the Baikal Rift Zone: evidence from a seismic refraction profile across southern Lake Baikal. J. Geophys. Res. Solid Earth 114, B08306.
Peng, J., Huang, J., Liu, Z., Xing, K., 2020. Constraints on S-wave velocity structures of the lithosphere in mainland China from broadband ambient noise tomography. Phys. Earth Planet. Inter. 299, 106406.
Shan, B., Xiong, X., Zhao, K., Xie, Z., Zheng, Y., Zhou, L., 2017. Crustal and upper-mantle structure of South China from Rayleigh wave tomography. Geophys. J. Int. 208, 1643–1654.
Shen, W., Ritzwoller, M., Kang, D., Kim, Y., Lin, F., Ning, J., Wang, W., Zheng, Y., Zhou, L., 2016. A seismic reference model for the crust and uppermost mantle beneath China from surface wave dispersion. Geophys. J. Int. 206, 954–979.
Shen, X., Kind, R., Huang, Z., Yuan, X., Liu, M., 2019. Imaging the Mantle Lithosphere below the China cratons using S-to-p converted waves. Tectonophysics 754, 73–79.
Shu, L., 2012. An analysis of principal features of tectonic evolution in South China Block. Geol. Bull. China 31 (7), 1035–1053 (in Chinese).
Shu, L., Zhou, X., Deng, P., Wang, B., Jiang, S., Zhao, X., 2009. Mesozoic tectonic evolution of the Southeast China Block: New insights from basin analysis. J. Asian Earth Sci. 34, 376–391.
Shu, L., Wang, B., Cawood, P., Santosh, M., Xu, Z., 2015. Early Paleozoic and early Mesozoic intraplate tectonic and magmatic events in the Cathaysia Block, South China. Tectonics 34, 1600–1621.
Tian, X., Zelt, C., Wang, F., Jia, S., Liu, Q., 2014. Crust structure of the North China Craton from a long-range seismic wide-angle-reflection/refraction data. Tectonophysics 634, 237–245.
Vidale, J.E., 1988. Finite-difference calculation of travel times. Bull. Seismol. Soc. Am. 78, 2062–2076.
Vidale, J.E., 1990. Finite-difference calculation of traveltimes in three dimensions. Geophysics 55, 521–526.
Wang, M., Chen, Y., Liang, X., Xu, Y., Fan, Y., Xu, T., Zhang, Z., Teng, J., 2015. Surface wave tomography for South China and the northern South China Sea area. Chin. J. Geophys. 58 (6), 1963–1975 (in Chinese).
Wang, Y., Zhang, A., Fan, W., Zhang, Y., Zhang, Y., 2013. Origin of paleosubduction-modified mantle for Silurian gabbro in the Cathaysia Block: Geochronological and geochemical evidence. Lithos 160-161, 37–54.
Wei, Z., Chen, L., Li, Z., Ling, Y., Li, J., 2016. Regional variation in Moho depth and Poisson's ratio beneath eastern China and its tectonic implications. J. Asian Earth Sci. 115, 308–320.
Xu, X., O'Reilly, S., Griffin, W., Wang, X., Pearson, N., He, Z., 2007. The crust of Cathaysia: Age, assembly and reworking of two terranes. Precambrian Res. 158, 51–78.
Ye, Z., Li, Q., Gao, R., Guan, Y., He, R., Wang, H., Lu, Z., Xiong, X., Li, W., 2013. Seismic receiver functions revealing crust and upper mantle structure beneath the continental margin of southeastern China. Chin. J. Geophys. 56 (9), 2947–2958 (in Chinese).
Ye, Z., Li, Q., Gao, R., Zhang, H., He, R., Wang, H., Li, W., 2014. A thinned lithosphere beneath coastal area of southeastern China as evidenced by seismic receiver functions. Sci. China Earth Sci. 57, 2835–2844 (in Chinese).
Zelt, C.A., 1999. Modelling strategies and model assessment for wide-angle seismic traveltime data. Geophys. J. Int. 139, 183–204.
Zelt, C.A., Smith, R.B., 1992. Seismic traveltime inversion for 2-D crustal velocity structure. Geophys. J. Int. 108, 16–34.
Zhang, G., Guo, A., Wang, Y., Li, S., Dong, Y., Liu, S., He, D., Cheng, S., Lu, R., Yao, A., 2013a. Tectonics of South China continent and its implications. Sci. China Earth Sci. 56, 1804–1828 (in Chinese).
Zhang, J., Zheng, Y., Zhao, Z., 2009. Geochemical evidence for interaction between oceanic crust and lithospheric mantle in the origin of Cenozoic continental basalts in east-Central China. Lithos 110, 305–326.
Zhang, Y., Chen, L., Ai, Y., Jiang, M., Xu, W., Shen, Z., 2018. Lithospheric structure of the South China Block from S-receiver function. Chin. J. Geophys. 61, 138–149 (in Chinese).
Zhang, Y., Shi, D., Lü, Q., Xu, Y., Xu, Z., Yan, J., Chen, C., Xu, T., 2021. The crustal thickness and composition in the eastern South China Block constrained by receiver functions: Implications for the geological setting and metallogenesis. Ore Geol. Rev. 130. https://doi.org/10.1016/j.oregeorev.2021.103988.
Zhang, Z., Wang, Y., 2007. Crustal structure and contact relationship revealed from deep seismic sounding data in South China. Phys. Earth Planet. Inter. 165, 114–126.
Zhang, Z., Badal, J., Li, Y., Chen, Y., Yang, L., Teng, J., 2005. Crust-upper mantle seismic velocity structure across southeastern China. Tectonophysics 395 (1), 137–157.
Zhang, Z., Xu, T., Zhao, B., Badal, J., 2013b. Systematic variations in seismic velocity and reflection in the crust of Cathaysia: New constraints on intraplate orogeny in the South China continent. Gondwana Res. 24, 902–917.
Zhao, Z., Dai, L., Zheng, Y., 2013. Postcollisional mafic igneous rocks record crust-mantle interaction during continental deep subduction. Nat. Sci. Rep. 3, 3413.
Zheng, J., Lee, C., Lu, J., Zhao, J., Wu, Y., Xia, B., Li, X., Zhang, J., Liu, Y., 2015. Refertilization-driven destabilization of subcontinental mantle and the importance of initial lithospheric thickness for the fate of continents. Earth Planet. Sci. Lett. 409, 225–231.
Zhou, X., Li, W., 2000. Origin of late Mesozoic igneous rocks in southeastern China: Implications for lithosphere subduction and underplating of mafic magmas. Tectonophysics 326 (3–4), 269–287.
Zhou, X., Sun, T., Shen, W., Shu, L., Niu, Y., 2006. Petrogenesis of Mesozoic granitoids and volcanic rocks in South China: a response to tectonic evolution. Episodes 29 (1), 26–33.
Zhu, R., Chen, L., Wu, F., Liu, J., 2011. Timing, scale and mechanism of the destruction of the North China Craton. Sci. China Earth Sci. 2011 (54), 789–797 (in Chinese).
Zhu, R., Xu, Y., Zhu, G., Zhang, H., Xia, Q., Zheng, T., 2012. Destruction of the North China Craton. Sci. China Earth Sci. 2012 (42), 1135–1159 (in Chinese).